MIRSURG

Mid-Infrared Solid-State Laser Systems for Minimally Invasive Surgery

Grant agreement no.: 224042

Specific Targeted Research
Theme 3: **Information and Communication Technologies (ICT)**

D3.6: Cascaded ns OPOs generating at 6.45 µm

Due date of deliverable: month 36
Actual submission date: month 41

Start date of project:	01/06/2008
Duration:	42 months
Organisation name of lead contractor for this deliverable:	KTH Royal Institute of Technology

Project co-funded by the European Commission within the Seventh Framework Programme (2008-2011)		
Dissemination Level		
PU	Public	PU
PP	Restricted to other programme participants (including the Commission Services)	
RE	Restricted to a group specified by the consortium (including the Commission Services)	
CO	Confidential, only for members of the consortium (including the Commission Services)	

Contents

1. Purpose and scope of the deliverable

This deliverable reports on the results achieved in nanosecond optical parametric cascaded scheme built according to the objective X of WP3. The cascaded scheme operating at 6.45 µm is an extension of the previous effort reported in Annual reports of 2009, 2010, deliverable D3.5 and also takes advantage of the work performed in WP1 as reported in deliverable D1.7. The parametric source reported in this deliverable gives access to the intermediate pulse lengths, those between few picoseconds as in deliverable D3.3 and tens of nanoseconds as in deliverable D3.7. Assessing advantages or disadvantages of this regime of operation for the applications in minimally invasive surgery are outside the scope of this deliverable. Nevertheless we will discuss briefly these issues in the introductory part below.

2. Introduction

Standard laser sources used in surgical applications exploit rapid buildup of the water vapour pressure with resulting fast expansion to the laser-heated volume to produce tissue ablation. Such lasers operate at 2 µm and 3 µm water absorption bands. Minimally invasive surgery requires minimization of collateral thermal damage in the tissue surrounding laser incision. Recent investigations employing 5 µs macropulses derived from a free-electron-laser (FEL) tuned to spectral 6.1-6.45 µm region where there is partial coincidence of the liquid water and amide-I and amide-II absorption indicate that the tissue ablation threshold and therefore total thermal exposure can be reduced with concomitant reduction in collateral damage [1]. Moreover, investigations of refractive laser surgery revealed that reduction of the laser pulsewidth to below 10 ns reduces further the collateral damage and ablation threshold fluence due to more prominent role of photoelastic tissue response as opposed to photothermal response which is dominant for longer pulses [2].

In this work we demonstrate all-diode-pumped 5 ns cascaded parametric source with high spatial beam quality and tunable in 6.27-8.12 µm range. The concept uses well-established and robust Q-switched laser at 1.064 µm to pump degenerate 2 µm master-oscillator power amplifier (MOPA) taking advantage of large aperture periodically poled Rb:$KTiOPO_4$ (PPRKTP) crystals [3] due to their high nonlinearity and volume Bragg grating (VBG) for spectral control [4]. The MOPA serves as a pump for a compact 3-dimensional RISTRA cavity $ZnGeP_2$ (ZGP) OPO [5] generating high-spatial quality tunable beam in the 6.27-8.12µm range. The RISTRA cavity has been designed and built by ISL and joint experiments for this deliverable were performed at KTH facilities. The PPKTP crystals used in the cascaded system in this deliverable have been designed and fabricated in WP1 of MIRSURG (deliverable D1.7). The ZGP crystals used in the second OPO cascade, converting 2 µm radiation to the tunable 6.27 – 8.12 µm output were acquired by ISL. Due to high cost of ZGP crystals and AR coatings, it was decided by ISL and KTH partners that the project resources would be more efficiently exploited if the same ZGP crystal and RISTRA cavity were used for the target 6.45 µm generation using both, the Q-switched Ho-laser system at ISL and in the cascaded OPO scheme at KTH.

3. Setup

The schematics of the experimental setup is shown in Fig. 1. The pump laser was a diode-pumped Q-switched single-frequency (seeded with a fiber DFB laser) Nd:YAG delivering 80 mJ, 10 ns – long linearly polarized pulses at 1064.4 nm with repetition rate of 100 Hz. The laser output was split by a thin-film polarizer P1 into two channels, one powering master OPO, while the other was used to pump PPRKTP parametric amplifier. The pump pulse energy at the moment of experiments was limited by large depolarization loss and decreased diode pumping efficiency owing to deficiencies in the design of the laser pump chamber. Subsequently the laser was refurbished by the manufacturer to deliver 210 mJ linearly polarized pulses. However the experiments with RISTRA cavity could not take advantage of increased pumping energy.

The 6.45 µm radiation is generated using ZGP OPO which has to be pumped with rather narrowband radiation at 2 µm, as shown in simulations presented in D3.5. As discussed there we use parametric master oscillator with VBG output coupler to lock the wavelength and to narrow the linewidth to about 1 nm. The OPO contained 10-mm long PPRKTP with optical aperture of 3mm x 5 mm and with domain period of 38.86 µm and the 20 mm–long cavity was formed by a plane incoupling mirror, highly reflective at 2.1 µm while highly transmitting at the pump wavelength. The VBG output coupler had reflectivity of

50% at 2.128 µm with the FWHM reflectivity bandwidth of 1 nm. Without the VBG, using 50% reflectivity dielectric mirror, the spectral width of the PPKTP OPO exceeds 100 nm around degeneracy and makes the cascaded pumping scheme very inefficient. The thin-film polarizer P3 and half-wave plate were employed to adjust the OPO pump power. The pump power was determined by two in general opposing requirements, i.e. the requirement of high enough output energy in order to efficiently extract the pump energy in the amplifier stage, which means running the parametric amplifier in deep saturation regime and at the same time limiting the master OPO pumping level in order to maintain good beam quality. The beam quality can deteriorate quite drastically in a linear OPO cavity with large Fresnel number when the OPO is driven more than two-times above the oscillation threshold. The reason for this is cascaded upconversion and downconversion cycles in the nonlinear OPO medium, which produces intensity-dependent spatial phase shifts.

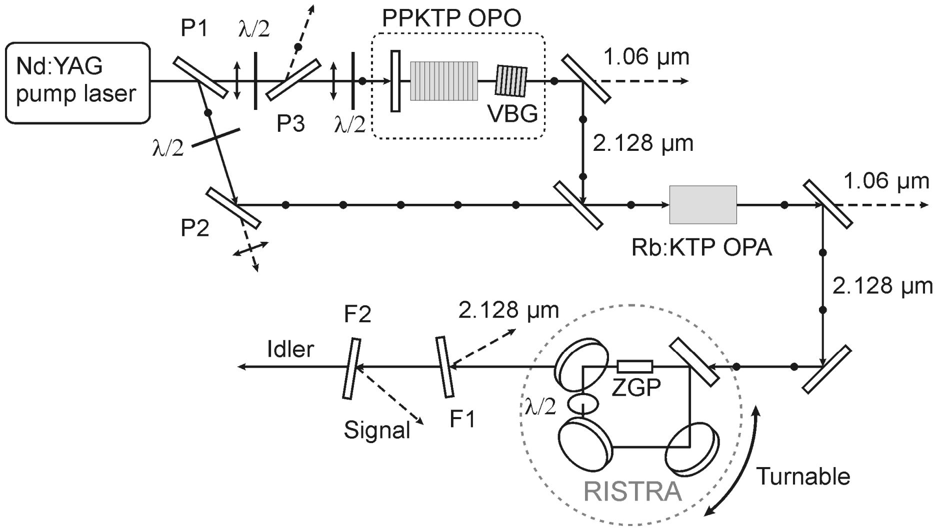

Fig. 1 Schematic setup of the cascaded parametric source generating 6.45 µm

The single-pass OPA contained 16 mm-long PPRKTP crystal with the same domain period as the one in the OPO but the optical aperture of 5 mm x 5 mm in order to accommodate the pump beam with a diameter of about 3 mm. Both PPRKTP crystals in the OPO and in the OPA as well as VBG were AR-coated for the pump and the parametric waves. The beam sizes of the OPA pump and seed were approximately matched using telescope in the OPA pumping arm. Nevertheless, it was somewhat difficult to compensate for remnant pump beam astigmatism without introducing spatial phase gradient which can be prominently imprinted in the OPA output beam intensity distribution, owing to the high-temporal and spatial coherence of the pump and the phase-sensitive nature of the parametric amplification.

Keeping in mind that the beam quality of the 6.45 µm radiation has to be of reasonably good quality in order to maximize the efficiency of fiber coupling, it was beneficial to exploit the image-rotating ring cavity design, so called RISTRA cavity [5]. ZGP crystal used in the final OPO stage is critically type-I phase matched where the pump at 2 µm has ordinary polarization wile the generated signal (3.18 µm) and the idler (6.45 µm) have extraordinary polarizations. In general for critically phase-matched interactions the produced beam is astigmatic and the beam propagation factor, M^2 , in the direction of Poynting vector walkoff is much lower than in the orthogonal direction. By arranging OPO in 3-dimensional ring-cavity configuration where cavity mirrors are arranged to rotate the image 90-degrees every roundtrip and incorporating a half-wave-plate in the cavity to restore the signal polarization the output beam astigmatism is removed and the beam propagation factor of the output beam is minimized. Moreover, for sufficiently large Poynting vector walkoff or long nonlinear crystal the quality of the output beam produced by RISTRA cavity becomes less sensitive to the pump beam quality.

The RISTRA cavity was built by ISL according to similar principles as described in Ref. 5. For operation in the range of 6 - 7 µm we employed type-I phase matching in 52.2°-cut ZGP. The crystal dimensions were 6 x 6 x 14 mm^3. The measured ZGP linear transmission at 2.128 µm was 92 %. The output coupler had a reflectivity of 65 % for the resonant signal and high transmittance for the idler, while all other mirrors were coated for high-reflectivity at the signal wavelength. The input coupler had about 19% reflection at the 2.128 µm pump wavelength. The coating on both sides of the ZGP created a single-pass loss of 17 % for the resonant signal wavelength at ~ 3.2 µm. The exit of the crystal had a reflectivity of 8 % for the idler wavelength at ~ 6.45 µm. The half-wave plate in the RISTRA cavity was a low order AR-coated MgF_2 and optimized for 2.9 µm. The lab arrangement of the cascaded 2 µm MOPA and the 6.45 µm RISTRA OPO is shown in Fig. 2. For the system alignment and characterization of the mid-infrared beams we employed pyroelectric camera (Spricon). The spectra of the RISTRA output were measured using Jobin-Yvon HR550i grating spectrometer.

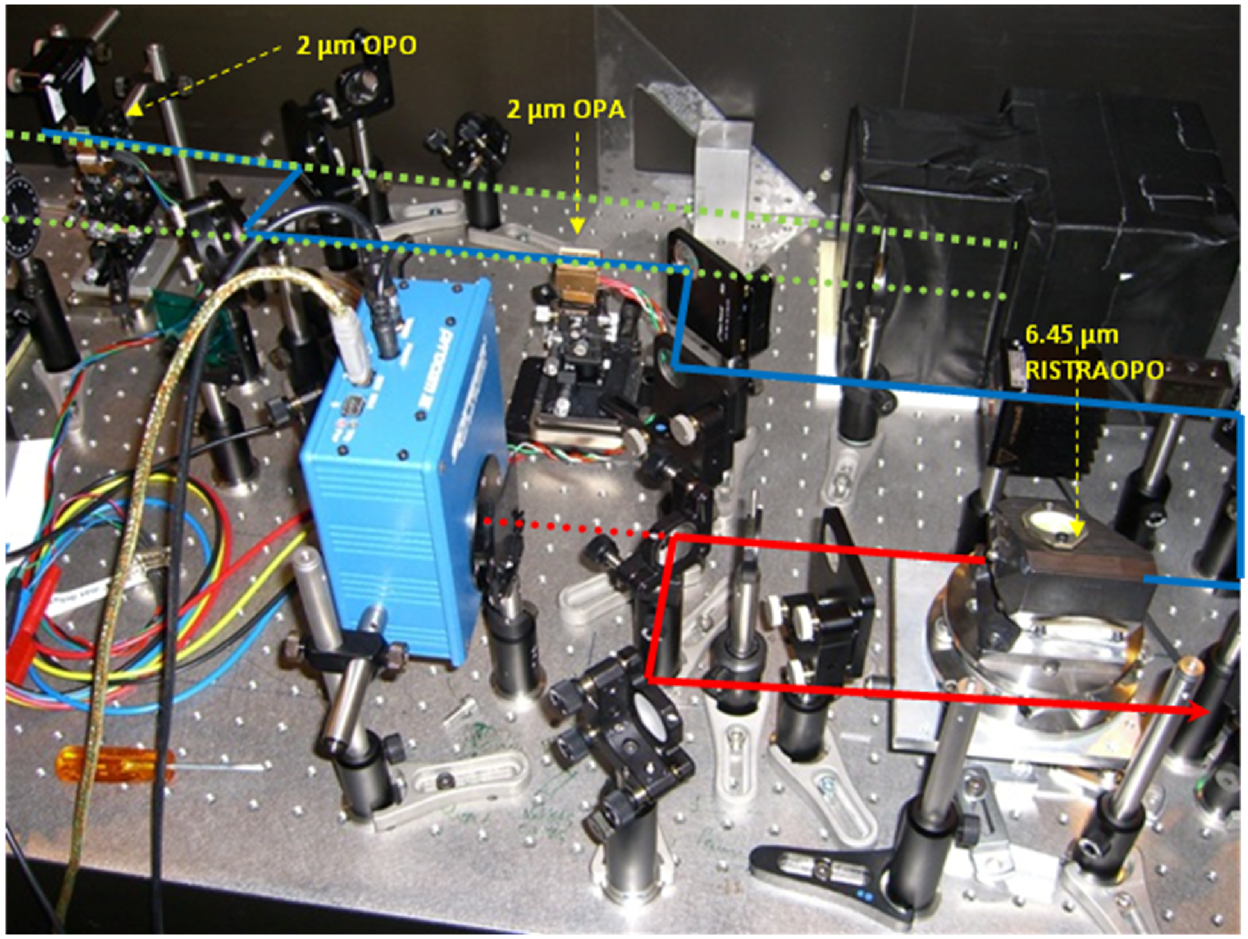

Fig. 2 Lab setup of the cascaded parametric source consisting of 2 µm master OPO-power OPA pumped at 1.064 µm and ZGP RISTRA OPO producing 3.18 µm and 6.45 µm radiation. The 1.064 µm beams are marked in green, 2 µm beams in blue, and the RISTRA output beams – in red.

4. The system performance

The PPKTP OPO VBG-locked at 2.128 µm generated 3.6 mJ, 8 ns pulses two-times above the oscillation threshold. This was chosen as the operation point for the master OPO due to the above-mentioned tradeoffs, although the efficiency at this point has not reached its maximum. The master OPO beam was superimposed on the dichroic mirror just before the PPKTP OPA stage. The OPA was pumped with 60 mJ pulses at 1.064 µm.

For seeding the OPA stage we used 3.6 mJ pulse energy from the OPO with the pulse length of about 8 ns. At the maximum available pump energy of 60 mJ the OPA generated 26 mJ giving the amplification factor of 7.2 and the energy extraction efficiency of 43%. The output energy dependence on the pump pulse energy for the 2 µm MOPA is shown in Fig. 3. Inset in the Fig. 3 shows MOPA output beam profile at maximum pump power. The intensity modulation apparent in the beam occurs due to spatial pulse front tilt introduced by the astigmatism compensating arrangement in the OPA pump beam. Due to the fact that both the 2 µm OPO and power OPA operate at degeneracy the phase-sensitive nature of the parametric amplification transfers the spatial phase modulation of the pump onto the intensity modulation of the

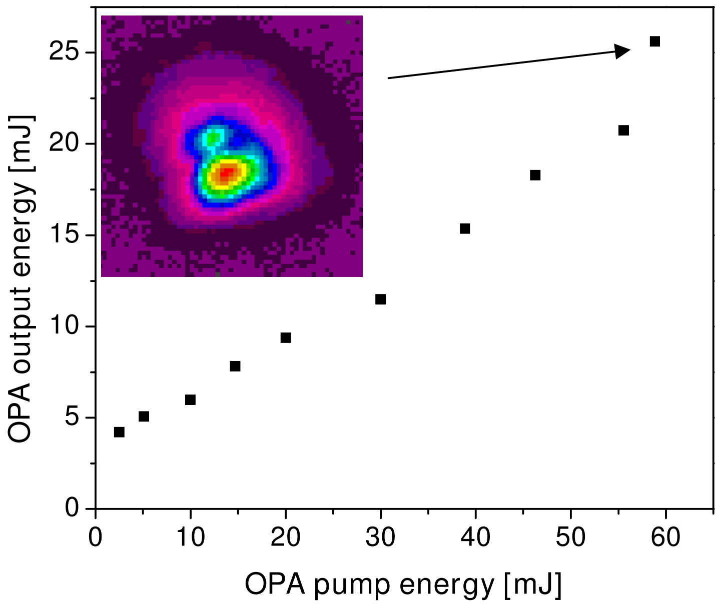

Fig. 3. Output energy of the 2.128 µm MOPA as a function of pump energy. Inset: output intensity profile of the MOPA.

MOPA output. A simple method for avoiding such modulation is by using a single astigmatism compensation scheme for both the OPO and the OPA. On the other hand, the remnant intensity modulation in the 2 µm beam proved not to be detrimental for the beam quality of 6.45 µm OPO due to the above mentioned properties of the RISTRA cavity. It should be mentioned that the pulse to pulse energy stability of the OPA output was similar to that of the pump, namely, about 1%.

The measured signal and idler output energies as a function of the 2.128 µm energy after the RISTRA incoupling mirror are shown in Fig. 4 and Fig. 5. For collinear alignment (the pump parallel to the resonated signal) RISTRA generated 6.27 µm idler and 3.22 µm signal with corresponding maximum pulse energies of 0.84 mJ and 1.25 mJ, respectively (Fig. 4). The RISTRA design allowed output wavelength tuning by simply rotating cavity without any additional adjustments. For ±1-degree rotation from the collinear position the idler tuned between 6.27 µm and 8.12 µm with the corresponding signal tuning between 3.22 µm and 2.88 µm (see Fig. 6). The noncollinear RISTRA performance corresponding to the idler at 6.45 µm, coinciding with the amide-II absorption band of interest for the surgery applications, is shown in the right graph of Fig. 3. The idler energy here was 0.9 mJ while the signal reached 1.4 mJ (Fig. 5).

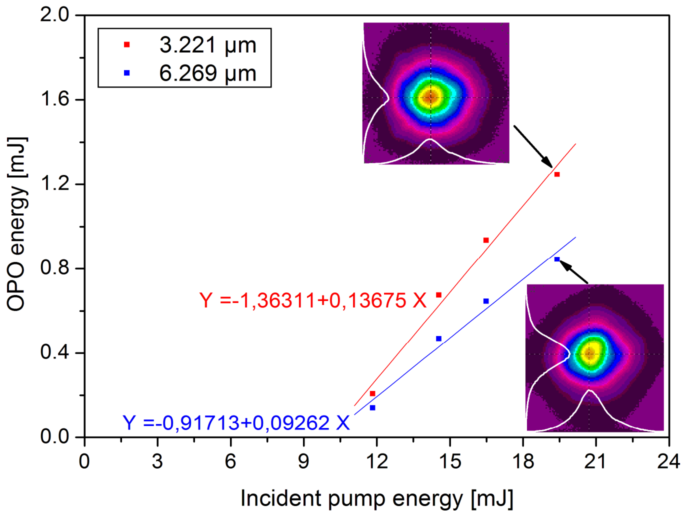

Fig. 4. Signal and idler energies of collinear RISTRA ZGP OPO. Insets: signal and idler intensity profiles.

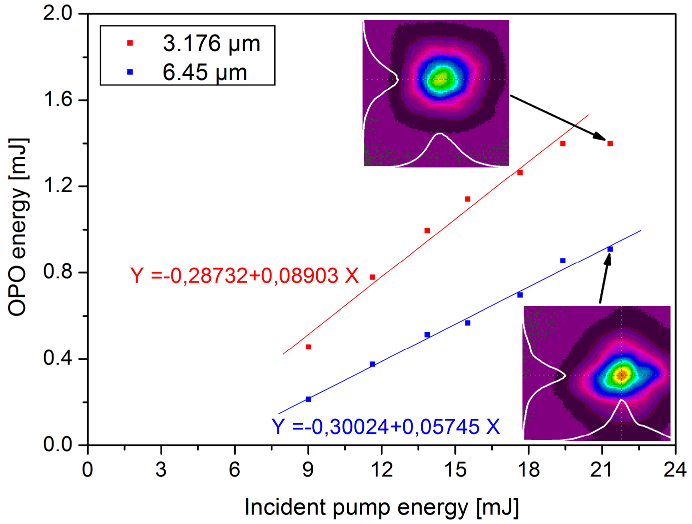

Fig. 5. Signal and idler energies of noncollinear RISTRA ZGP OPO. Insets: signal and idler intensity profiles.

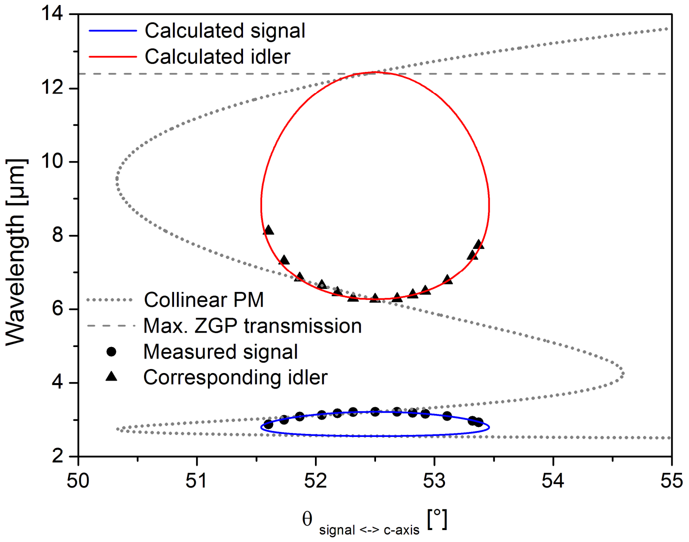

Fig. 6. Signal and idler angle-tuning characteristics in RISTRA ZGP OPO. Dashed line: collinear type-I phase matching; Data points: measured signal and idler wavelengths as function of RISTRA cavity rotation angle; Solid lines: calculated noncolinear phase matching.

The measured signal pulse length was about 5 ns. As shown in Fig. 4 and Fig. 5 the signal and idler beam intensity profiles were very smooth although some astigmatism appeared for noncollinear operation. High-spatial quality of the output beams is a well documented property of the image-rotating RISTRA design and is of high importance for parametric sources deemed for minimally invasive surgery where the beam focussability is rather important.

5. Conclusions

The realized cascaded parametric source generates the wavelengths targeted by the MIRSURG project. The peak power of the idler at 6.45 µm was 180 kW, while that of the signal at 3.178 µm – 280 kW produced at a repetition rate of 100 Hz from all-diode pumped system. The pulse energy of 0.9 mJ at 6.45 µm is almost 4-times higher than the reported model tissue ablation threshold of 0.25 mJ for 100 ns pulses at this wavelength [6]. As mentioned in the introduction there is indication that sub-10 ns pulse would be actually beneficial for minimally invasive surgery. Probably, the signal output can also be exploited for surgery applications. The overall system performance in terms of efficiency can be further increased and the output power scaled up by increasing the 1.064 µm pump pulse energy by refurbishing the pump laser. The limitation for increasing the average power might be the remnant absorption of 2 µm radiation in ZGP and the associated thermal lens which might render relatively long RISTRA cavity unstable.

6. References

[1] G.S. Edwards, R.H. Austin, F.E. Carroll, M.L. Copeland, M.E. Couprie, W.E. Gabella, R.F. Haglund, B.A. Hooper, M.S. Hutson, E.D. Jansen, K.M. Joos, D.P. Kiehart, I. Lindau, J. Miao, H.S. Pratisto, J.H. Shen, Y. Tokutake, A.F.G. van der Meer, and A. Xie, "Free-electron-laser-based biophysical and biomedical instrumentation", Rev. Sci. Instr., **74**, 3207 (2003).

[2] W. B. Telfair, C. Bekker, H. J. Hoffman, P. R. Yoder, Jr., R. E. Nordquist, R. A. Eiferman, and H. H. Zenzie, “Histological comparison of corneal ablation with Er:YAG laser, Nd:YAG optical parametric oscillator, and excimer laser,” J. Refractive Surgery, **16**, 40-50 (2000).

[3] A. Zukauskas, N. Thilmann, V. Pasiskevicius, F. Laurell, and C. Canalias “5 mm thick periodically poled Rb-doped KTP for high energy optical parametric frequency conversion” Opt. Mat. Express, **1**, 201-206 (2011).

[4] M. Henriksson, L. Sjöqvist, V. Pasiskevicius and F. Laurell, “Mode Spectrum of Multi-Longitudinal Mode Pumped Near-Degenerate OPOs with Volume Bragg Grating Output Couplers” Opt. Express, **17**, 147582-17589 (2009).

[5] A. Dergachev, D. Armstrong, A. Smith, T. Drake, and M. Dubois, "3.4-µm ZGP RISTRA nanosecond optical parametric oscillator pumped by a 2.05-µm Ho:YLF MOPA system", Opt. Express, **15**, 14404-14413 (2007).

[6] M. A. Mackanos, D. Simanovskii, K. J. Joos, H. A. Schwettman, and E. D. Jensen, ”Mid infrared optical parametric oscillator as a viable alternative to tissue ablation with the free electron laser,” Lasers in Surgery and Medicine, Vol. 39, pp. 230-236, 2007.